Journal of Microscopy and Ultrastructure 1 (2013) 65–75

Contents lists available at ScienceDirect

Journal of Microscopy and Ultrastructure

journal homepage: www.elsevier.com/locate/jmau

Review

Advanced endoscopic imaging technologies for in vivo cytological examination of gastrointestinal tract lesions: State of the art and proposal for proper clinical application

Antonello Forgione[a,b,*], Salman Yousuf Guraya[c]

[a] AIMS Advanced International Mini-invasive Surgery Academy, Milan, Italy
[b] Department of General and Emergency Surgery, Niguarda Cà Granda Hospital, Milan, Italy
[c] College of Medicine, Taibah University, Almadinah Almunawwarah, Saudi Arabia

ARTICLE INFO

Article history:
Received 1 November 2013
Accepted 22 November 2013

Keywords:
In vivo cytology
Narrow band imaging
Autofluorescence imaging
Confocal laser imaging
Optical coherence tomography
Endocytoscopy
Endoscopic ultrasound

ABSTRACT

Since its introduction, conventional endoscopy has changed the management framework of a variety of gastrointestinal tract (GIT) diseases and is now considered a fundamental component in the evaluation and treatment of gastrointestinal diseases. Histologic analysis of specimens remains the gold standard for the final diagnosis of gastrointestinal lesions. However, such workup is time-consuming and labor-intensive. This restricts the endoscopists to immediately determine the necessity for resection during ongoing endoscopies, necessitating the need to repeat the procedure. Furthermore, overtreatment (resection of benign lesions) or undertreatment (biopsy instead of resection for neoplastic tissue) can lead to frustrations, unnecessary risks (e.g., bleeding) for the patients, and delay in definite treatment for the urgent cases.

Recently, developments in endoscopic and imaging technologies (narrow-band imaging, autofluorescence imaging, confocal laser endoscopy and imaging, optical coherence tomography, and endoscopic ultrasound) can provide a wide variety of valuable tools for in vivo cytological diagnosis of neoplastic lesions of GIT, even beyond inner layer of the bowel. Such investigations, may therefore lead to an optimized rapid diagnosis of GIT lesions, providing important implications also for immediate therapy, during ongoing endoscopies (e.g., endoscopic resection of neoplastic tissue). Moreover the possibility to properly investigate in vivo progression of the extraluminal disease (lymph node status) allows reducing, if not eliminating the need of extensive resection just for proper staging.

The present review convincingly describes the operating systems of each diagnostic modality, their clinical implications, and future vision of the role of these modern tools in the clinical diagnosis of GIT diseases.

* Corresponding author at: AIMS Advanced International Mini-invasive Surgery Academy, Piazza Ospedale Maggiore 3, 20162 Milan, Italy. Tel.: +39 0264447605.
E-mail addresses: antonello.forgione@aimsacademy.org, antonello.forgione@gmail.com (A. Forgione).

2213-879X
http://dx.doi.org/10.1016/j.jmau.2013.11.001

Contents

1. Introduction

Despite a diverse range of emerging developments in gastrointestinal endoscopic techniques, early cancer can rarely be identified by routine examination. Worldwide, more than 350,000 new cases with cancer in oropharynx and hypopharynx are diagnosed and 197,000 annual deaths from these cancers are recorded [1,2]. Colorectal cancer remains one of the leading causes of cancer death in the western world [3,4] and develops in about 5–6% of the adult population; almost one half will die as a consequence of the disease [5]. The incidence and related mortalities from colorectal carcinoma have been steadily increasing in the Kingdom of Saudi Arabia over the past twenty years [6]. Such alarming data demands attention to the novel developments in diagnostic armamentarium, with high accuracy, feasibility, and effectiveness. The present review outlines the modern technologies with possibilities of in vivo cytological analysis, permitting rapid diagnosis and treatment strategies.

2. Narrow band imaging

Narrow band imaging (NBI) is a new optical technology that can clearly visualize the microvascular structure of the organ surface [7]. Machida et al. performed endoscopic evaluation of the colonic lesions (by using conventional colonoscopy, NBI colonoscopy, and chromoendoscopy) focusing on mucosal pit pattern and the shape of colonic crypt orifices [8]. NBI was able to clearly distinguish between neoplasia and non-neoplastic lesions according to the pit patterns (following Kudo's classification types 1 and II were non-neoplastics and III and IV were neoplastic). All suspected lesions were subjected to histological examination and the results were compared with the endoscopic findings. The accuracy of endoscopic diagnosis compared with histological findings was 79.1% and 93.4% with conventional and NBI colonoscopy, respectively. This finding underpins the diagnostic accuracy of NBI, which elaborates its future role in the detection of GIT lesions.

2.1. Operating system

NBI involves the placement of narrow-band filters in front of a conventional white light source to capture tissue illumination at selected narrow wavelength bands. The propagation of light depends on its wavelength Blue, having a shorter wavelength, diffuses in a smaller range, whereas red, possessing a longer wavelength, diffuses widely and deeply. The blue filter is designed to correspond to the peak absorption spectrum of hemoglobin to emphasize the image of capillary vessels on surface mucosa [9–12]. The NBI systems currently available use 2 narrow-band filters that provide tissue illumination in the green (540 nm) and blue (415 nm) spectrum of light [13]. Deeper mucosal and submucosal vessels made visible by the 540-nm light appear cyan, whereas capillaries in the superficial mucosal layer are emphasized by the 415-nm light and appear brown (Fig. 1). The final composite NBI is reconstructed from the 415-nm image in the blue and green channels and the 540-nm image in the red channel of the monitor [14]. The NBI filter sets (415–30 nm, 445–30 nm, 500–30 nm) are selected to obtain fine images

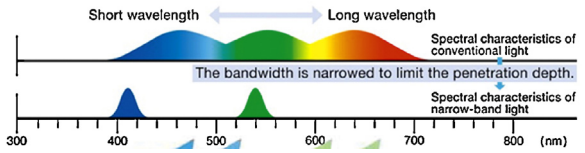

Fig. 1. Narrow Banding Imaging (NBI) physical basis.

of the microvascular structure. Because the 415-nm is the hemoglobin absorption band, the thin blood vessels such as capillaries on the mucosal surface can be seen most clearly on this wavelength [15]. Light with short wavelength is within the hemoglobin absorption band, so that blood vessels may be demonstrated with sufficient contrast against the normal background [14,15].

2.2. Clinical applications

Per se, GIT malignancies originate from the gastrointestinal mucosa, which necessitates precise endoscopic evaluation to detect early lesions, before they progress to an advanced stage (Fig. 2A and B). NBI is useful in elaborating the following:

2.2.1. Increased microvessels in the neoplastic epithelium

Angiogenic features of the GIT neoplastic lesions is a hallmark of NBI endoscopy, which illustrates increased microvessels in the neoplastic epithelium, whereas normal epithelium contains few microvessels [16]. Microcapillary vessels in normal mucosa or on the surface of hyperplastic lesions are arranged in a honeycomb pattern around mucosal crypts without any change in vessel diameter, but the capillaries in neoplastic lesions become elongated with larger diameters as the number and density of microcapillary vessels increase during the transition from premalignant to malignant lesions [17]. Sano et al. labeled the mucosal capillary mesh arranged in a honeycomb pattern around mucosal crypts as 'meshed capillary vessels' [18]. By identifying meshed capillary vessels pattern, the researchers were able to develop a sequential method using NBI for more frequent detection of abnormal microcapillaries as indicators of neoplasia.

A recent study using NBI with magnification, the microvascular architecture observed on the surface of the detected lesions, capillary patterns (CP), was divided into non-neoplastic (CP I) and neoplastic (CP II and CP III) types [19]. Ninety-seven per cent ($N = 103$) of colorectal neoplastic lesions with CP II were histologically diagnosed as low-grade dysplasia. Eighty-seven per cent ($N = 31$) of the colorectal neoplastic lesions with CP III were high-grade dysplasia or invasive cancer.

2.2.2. Carcinoma in situ of the oropharynx and hypopharynx

Muto et al., by using NBI, examined the upper GIT lesions during routine endoscopic screening and surveillance of 600 individuals [7]. More than 50 superficial lesions could be detected by NBI. Among them, 41 superficial lesions were endoscopically removed; twenty-nine lesions were histologically confirmed to be carcinoma in situ, and the remainder exhibited cancer with microinvasion beneath the epithelium (Fig. 2A and B).

2.2.3. Colonic adenoma detection

A study reported that NBI produces greater color contrast between adenomas and the surrounding normal mucosa than does the white light used in conventional imaging [20]. Imaged in blue light, blood vessels on the surface of polyps, particularly adenomas, generate a sharp color contrast with the surrounding normal mucosa, which can enhance detection of lesions. The pan-colonic NBI system improves the total number of adenomas detected, including significantly more diminutive adenomas, without prolongation of extubation time. These results indicate that routine use of the NBI system for surveillance of diminutive adenomas may be recommended [16].

2.2.4. Early colorectal neoplasia

Katagiri et al. conducted a prospective study to evaluate whether different CP (CP type II and CP type III) visible during NBI with magnification provided sufficiently high reliability for distinguishing adenomas from intramucosal and invasive cancers [19]. The overall diagnostic accuracy, sensitivity and specificity of their results were 95.5%, 90.3% and 97.1%, respectively.

2.2.5. Depth and extent of invasion of the colorectal cancer

Ikematsu et al. reported that the sensitivity, specificity and diagnostic accuracy of CP types IIIA and IIIB for differentiating intramucosal or slight submucosal invasion (<1000 mm from deep submucosal invasion) were 84.8%, 88.7% and 87.7%, respectively [21]. This information provides a valuable roadmap for surgeons and physicians to devise a multi-disciplinary treatment strategy for colorectal cancer.

3. Autofluorescence imaging

Autofluorescence imaging (AFI) may detect dysplasia and neoplasia in upper GIT lesions especially in Barrett's esophagus. In AFI, tissue is illuminated with a light source, mostly in the near-UV to green range of the spectrum, and images of the fluorescence produced in the tissue are altered by absorption, and scattering events are recorded using a camera [22]. When AFI is used, nondysplastic Barrett's esophagus appears green, whereas dysplastic or neoplastic lesions appear blue or violet. In addition to its role in identifying gastrointestinal neoplasia, AFI has an established role in diagnosing a wide range of ophthalmological diseases [23]. The use of fluorescent contrast medium is another viable option in AFI.

3.1. Operating system

The autofluorescence endoscopy system (Olympus Optical Co., Ltd., Tokyo, Japan) includes a high-resolution videoendoscope and an AFI technology. It has a xenon light source, with a rotary red/green/blue band-pass filter. With this light source, the mucosa is sequentially illuminated with red, green, and blue light at a frequency of

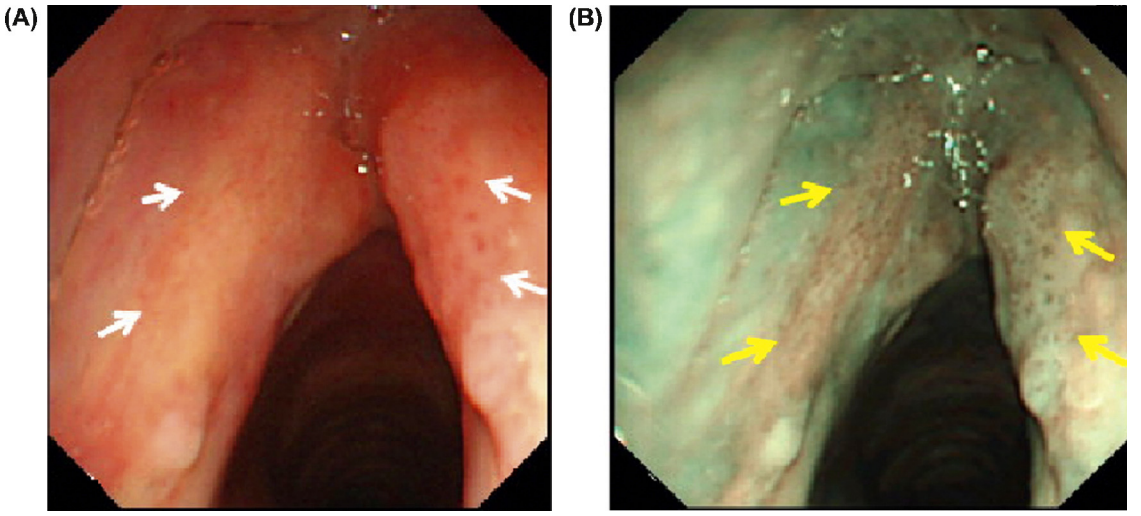

Fig. 2. (A) Conventional endoscopic view. (B) NBI view.

20 cycles per second [24]. The high-resolution videoendoscope in this system has two separate monochromatic charge-coupled devices; one for white-light endoscopy (WLE), and one for AFI (Fig. 3). In the WLE mode, the reflected red, green, and blue light is detected by the standard charge-coupled devices and is converted to an electronic signal that is passed to the videoprocessor. The processor electronically overlays the red, green, and blue signals to produce high-quality white-light images. WLE and AFI can be alternated by means of a switch located conveniently on the endoscope. During endoscopic examination, still images of all suspicious lesions are taken, following 2–4 biopsies from each area.

3.2. Clinical applications

Since the discovery of the potential of AFI for the detection of oral cancer, many evidence-based studies have been performed for the oral cavity and the rest of the upper aerodigestive tract especially Barrett's esophagus (Fig. 4A and B). This technique has demonstrated great promise in the following aspects [25]:

(1) Capability in providing a higher contrast between a lesion and (surrounding) healthy tissue than white light inspection.
(2) Ability in differentiating between different types of lesions, in particular benign, dysplastic and malignant.
(3) Efficacy in identifying unknown lesions and unknown extensions of known lesions, which is useful for tumor demarcation

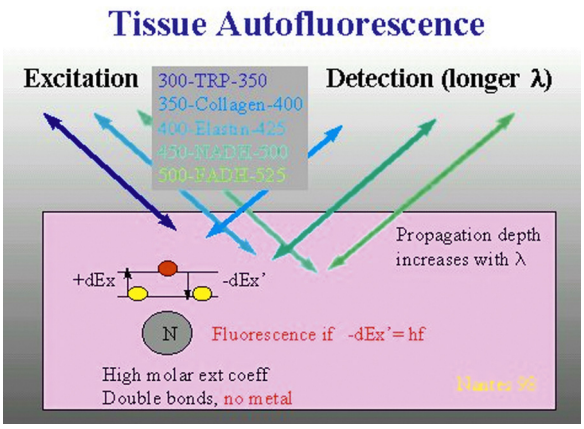

Fig. 3. Autofluorescence physical basis. Physical basis of autofluorescence imaging which utilizes xenon light source, with a rotary red/green/blue band-pass filter. With this light source, the mucosa is sequentially illuminated with red, green, and blue light at a frequency of 20 cycles per second

Kulapaditharom et al. examined 31 normal and 35 inflammatory sites; 4 granulomas, 15 dysplastic and 13 neoplastic lesions in the head and neck region through an endoscope using 442 nm excitation [26]. Out of these, 19 lesions were identified in the oral cavity, of which 8 were either dysplastic or neoplastic. Betz et al., by using 375–440 nm excitation for AFI, studied 30 patients with tumors of the oral mucosa or oropharynx, and reported sufficient to excellent demarcation by lower fluorescence intensity in 20 tumors [27]. However, 10 tumors were not distinguishable from their host tissues. These tumors were all located at the tongue, the soft palate or the tonsillar sinus. Generally, flat epithelial lesions were found to be outlined subjectively better by AFI than large, exophytic tumors. Although high sensitivities and specificities have been obtained using porphyrin-like fluorescence [28,29], other studies have claimed that red fluorescence is not specific for malignancies [30]. AFI has also been found to be an excellent tool in the diagnosis of precancerous and cancerous laryngeal lesions of the larynx [31].

4. Confocal laser endoscopy

The confocal laser endoscope (CLE) is a novel diagnostic tool to analyze living cells during endoscopic examinations,

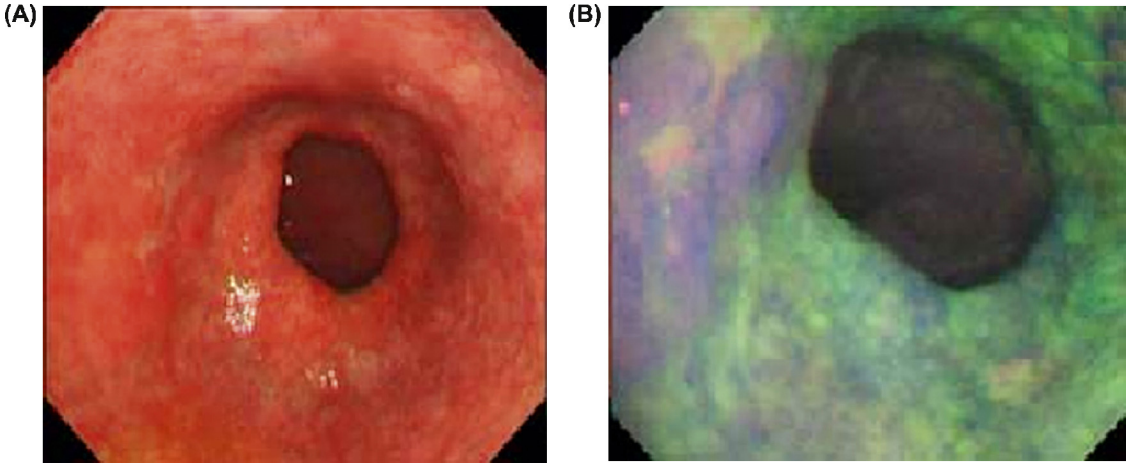

Fig. 4. (A) Conventional endoscopic view. (B) Endoscopic autofluorescence view of suspicious Barrett esophagus (blue violet area).

thus enabling virtual histology of neoplastic changes with high accuracy [32]. These emerging technologies may be of significant importance in clinical practice, and may lead to an accurate, reliable, and rapid in vivo diagnosis of neoplastic lesions.

4.1. Operating system

The components of the confocal laser colonoscope are based on incorporation of a confocal laser microscope in the distal tip of a conventional video colonoscope (EC3870K; Pentax, Tokyo, Japan), which enables confocal microscopy in addition to standard videoendoscopy (Fig. 5). Laser scanning confocal microscopy is an adaptation of light microscopy whereby focal laser illumination is combined with pinhole limited detection to geometrically reject out-of-focus light [32]. During laser endoscopy, an argon ion laser delivers an excitation wavelength of 488 nm, and confocal images are collected at a scan rate of 0.8 frames/s (1024 × 1024 pixels) or 1.6 frames/s (1024 × 512 pixels) (Fig. 5) [33].

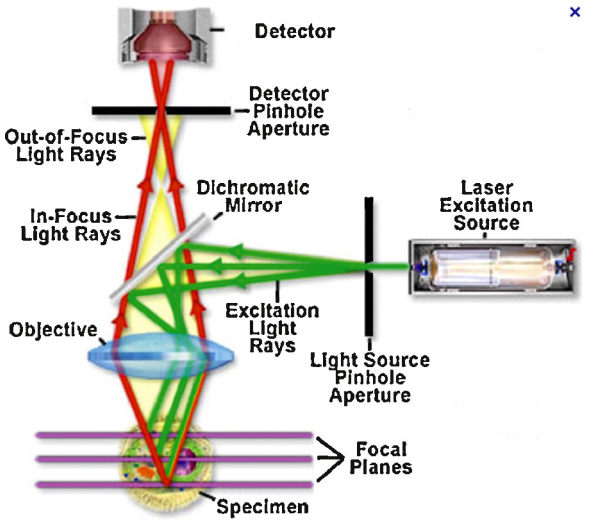

Fig. 5. Confocal laser microscopy physical basis. Confocal laser microscopy with illustration of its physical basis. This system integrates the adaptation oflight microscopy, where focal laser illumination is combined with pinhole-limited detection to geometrically reject out-of-focus light. An argon ion laser delivers an excitation wavelength of 488 nm, and confocal images are collected at a scan rate of 0.8 frames/s.

4.2. Clinical applications

Whereas the nuclei of the intestinal epithelial cells are not readily visible during confocal endoscopy because of the pharmacologic properties of fluorescein sodium, CLE demonstrates a more prismatic appearance of intestinal epithelial cells in vivo, as compared with formalin-fixed biopsy tissue, influenced by the absence of fixation artifacts. In the normal colon, CLE shows regular distribution of round-shaped crypts with round or oval crypt openings and a normal number of goblet cells. With CLE, intraepithelial neoplasm and colon cancers display tubular, villous, or irregular architecture with a reduced number or loss of goblet cells. A unique gap between the cells indicates loss of cellular junction due to loss of tight junctions as a potential sign of early malignancy [32]. Dilated and distorted vessels with marked leakage and irregular architecture with little or no orientation to adjunct tissue is another hallmark of malignancy (Fig. 6A and B).

During colonoscopy, CLE is first introduced into the terminal ileum or cecum, and a total of 5 mL fluorescein (5–10 mL of a 10% solution; Alcon Laboratories, Inc.) sodium and 2 mL butylscopolamine (Buscopan; Boehringer Ingelheim, Germany) is then given intravenously, because peristalsis may lead to artifacts. On withdrawal, all parts of the colon are examined systematically. Standardized locations (every 10 cm in the colon and the distal part of the ileum) and every macroscopically visible lesion are examined with the help of the CLE imaging system. Every flat or suspected lesion is stained before the confocal examination in a targeted fashion by using methylene blue at a final concentration of 0.1% to clarify the borders of the lesions. In addition, the distal 20 cm of the colon is stained in an untargeted fashion with methylene blue. After CLE, all patients develop a slight yellow coloration of the skin (a

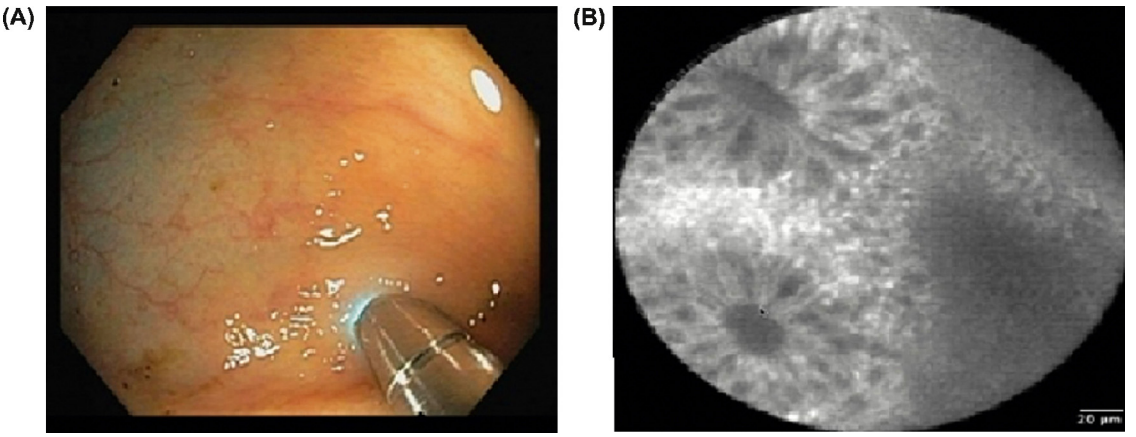

Fig. 6. (A) Endoscopic view of the probe. (B) Confocal microscopic view of the mucosa.

side effect of fluorescein sodium), which disappears in all cases within 60 min.

5. Optical coherence tomography

The technique of optical coherence tomography (OCT), by using fiber-optic probe, enables the acquisition of very high-resolution images, allowing imaging of individual cells. Such imaging is of a much higher resolution than is possible with other clinical modalities, such as CT, MRI or ultrasound, and is more similar to the level of detail achievable by histology [34].

5.1. Operating system

OCT is an interferometric imaging strategy that is analogous to ultrasound but implies near infrared light waves instead of sound waves. Light from a broadband source is split into two channels by an optical beam splitter [35]. First channel, the reference arm, is terminated by a mirror, which reflects light back along the path. Second channel, the sample arm, is weakly focused into the tissue sample under examination (Fig. 7). A small percentage of the light is backscattered from multiple depths within the tissue and captured by the system. Reflected light from the reference arm and backscattered light from the sample arm are combined, and light that has traveled the same optical path length in both arms, to within the short coherence length, is coherently interfered, giving a signal indicative of the backscatter from a particular depth in the tissue sample [36]. By varying the optical path length of the reference arm, we can attain the tissue backscatter at varying depths.

Endoscopic OCT probes typically consist of a length of single mode fiber encased in a protective plastic catheter. Attached to the distal end of the probe is focusing optics, often a small GRIN lens. Majority of the miniaturized probes described in the literature are side-facing, and will have some mechanism to deflect the light beam perpendicular to the axis of the probe, either through the use of a mirror or a prism via total internal reflection. In OCT contrast enhancement, backscatter enhancing contrast agents based on gold nanoparticles [37] and encapsulating microspheres containing scattering or absorbing nanoparticles are being developed [38].

5.2. Clinical applications

OCT, a non-invasive optical imaging technique, provides high-resolution cross-sectional images of tissue microstructure. By using OCT, early in vivo human research has shown its potential of differentiating between healthy and pathologic airway wall structure. Endoscopic OCT imaging showed normal bronchus to have a uniform layered structure. In contrast, areas of tumor showed a loss of this layered structure and a thickening of the epithelial surface, leading to thicker airway walls (probe diameter 1.5 mm, 4 B-scans/s, 16 lm axial resolution in air) [39]. Endoscopic OCT entails detailed imaging of the mucosal

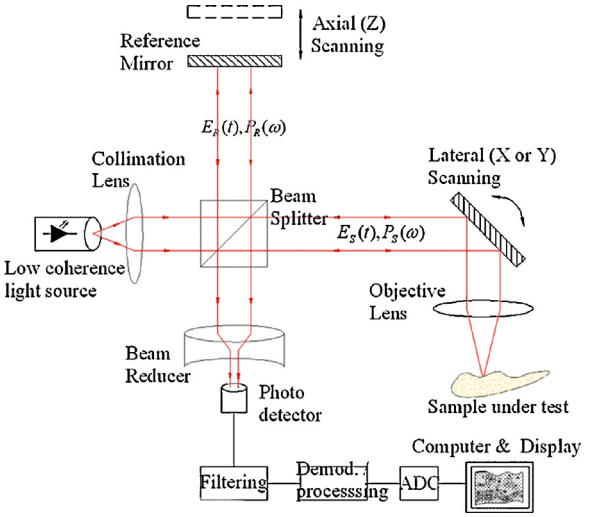

Fig. 7. Optical coherence tomography physical principle. Physical principles of optical coherence tomography, which implies near infrared light waves, which is split into two channels by an optical beam splitter. Reflected light and backscattered light are combined, and light that has traveled the same optical path length in both arms, to within the short coherence length, is coherently interfered, giving a signal indicative of the backscatter from a particular depth in the tissue sample.

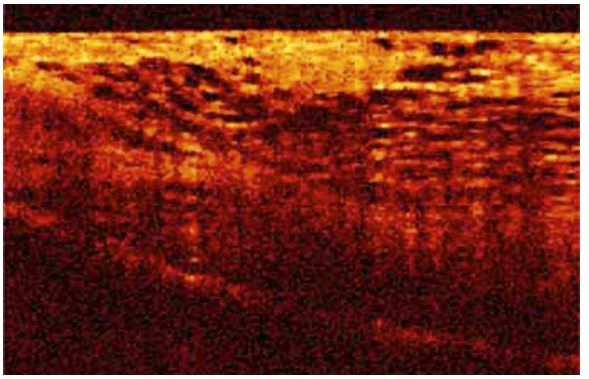

Fig. 8. OCT images of the inner layer of the bowel.

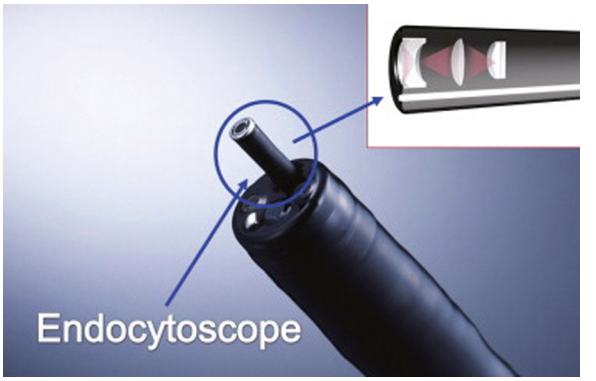

Fig. 9. Endocytoscope probe.

and submucosal structures of the human GIT (Fig. 8), and has also been demonstrated on the esophagus, stomach, duodenum, terminal ileum, colon and rectum [40,41], urinary tract [42], macular lesions [43], and coronary imaging [44]. In particular, there has been significant research in the application of endoscopic OCT probes to the diagnosis and monitoring of Barrett's esophagus [45].

Because the degree of OCT reflectivity depends upon nuclear size, a markedly inhomogenous and hyporeflective backscattering of the signal indicates disorganized tissue architecture and the presence of high-grade dysplasia. OCT features predictive of the presence of intestinal metaplasia are [46]:

(1) Absence of the layered structure of the normal squamous epithelium and the presence of the vertical crypt-and-pit morphology of normal gastric mucosa
(2) Disorganized architecture with inhomogeneous backscattering of the signal and an irregular mucosal surface
(3) Presence of submucosal glands characterized at the OCT image as pockets of low reflectance below the epithelial surface

These OCT criteria applied to images acquired prospectively, were found to be 97% sensitive and 92% specific for specialized intestinal metaplasia, with a positive predictive value of 84% [47]. Despite the potential of this technology, OCT imaging has been restricted in clinical applications by its extremely limited imaging depth, typically only 2–3 mm in tissue. Fiber bundles have been used to demonstrate endoscopic OCT applications, but equalizing delays across such a large number of fibers in a flexible bundle has proven problematic to date [48].

6. Endocytoscopy

Endocytoscopy, an ultra-high magnification technique, enables surface morphology to be assessed with magnifications in excess of 450× in real time [49]. This valuable device can be used throughout the GIT, enabling further characterization of pathology such as dysplasia or early cancer in Barrett's esophagus, villous and cellular morphology in patients with suspicion of celiac disease, or assessing and differentiating colonic polyps in real time.

Latest developments in technologies permits to perform microscopic imaging of living cells from both normal mucosa and malignant tissue in the GIT [50]. Endocytoscopy is a catheter-type contact endoscope that has more than 1000-fold magnifying power and can pass through the working channel of the straight-view endoscope (Fig. 9). The nucleus, cell body, and even the nucleolus can be clearly distinguished with high-resolution images, comparable with those of conventional cytology. This unique technology has the potential to provide in vivo histologic diagnoses during endoscopic examinations, similar to those obtained currently by conventional histology techniques.

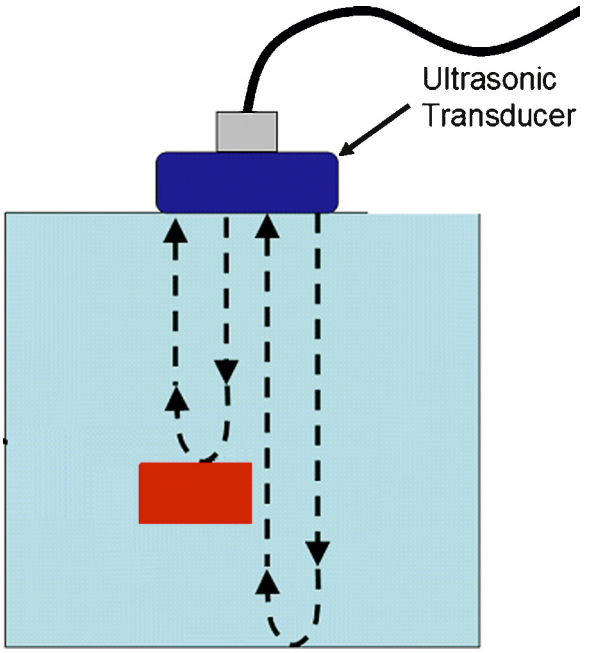

Fig. 10. Ultrasonography physical principle.

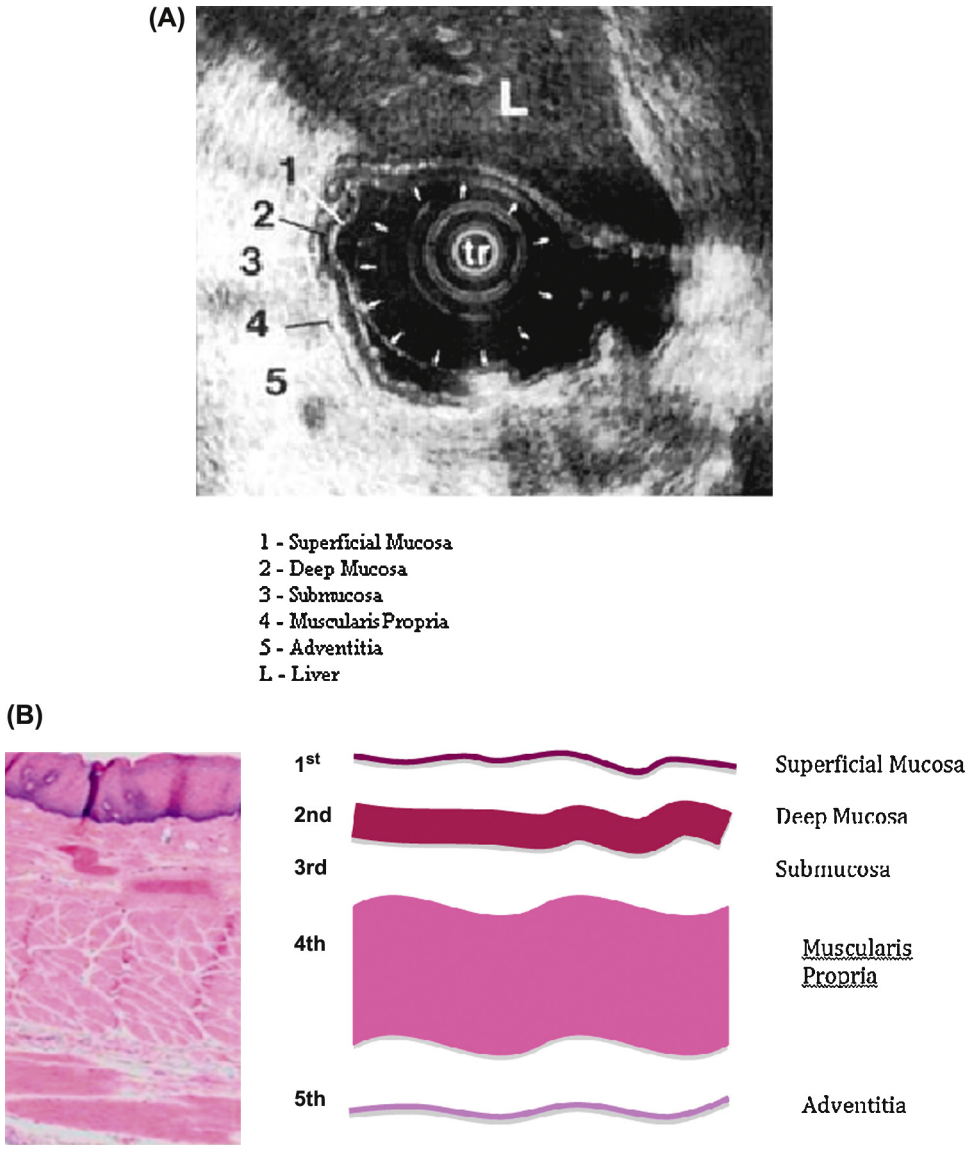

Fig. 11. (A) Endoscopic ultrasonographic features of intestinal mucosa. (B) Correspondence of bowel wall layers and EUS.

6.1. Operating system

The target tissue is first stained by the application of a double stain technique, which approximates hematoxylin and eosin staining in conventional histology. The target area is first treated with a mucolytic agent, 10% N-acetylcysteine, followed by an application of 1% methylene blue, which stains the nucleus, and 0.1% crystal violet, which stains nucleus as well as the cytoplasm. The endocytoscope probe is then maneuvered through the working channel and is gradually progressed until the tip approximates the mucosa.

6.2. Clinical applications

Potential applications of the endocytoscope include the identification of dysplastic or early cancerous lesions in premalignant conditions of the GIT, histological differentiation of serrated polyps [51] and inflammatory bowel disease (IBD) [52]. In IBD the following clinical implications of endocytoscopy have been reported:

(1) Differential histologic changes of Crohn's disease (CD) and Ulcerative colitis (UC) in vivo in real time, allowing for a targeted and tactical biopsy approach.
(2) Discrimination of mucosal inflammatory cells during endoscopy, thus determining the histopathologic activity of UC.
(3) Molecular imaging with fluorescence-labeled probes against disease-specific receptors, enabling individualized management of patients with IBD.

A study revealed similarities between endocytoscopic images and horizontal histologic pictures of cancerous and

normal squamous cells in the esophagus [53]. The obvious difference in nuclear and structural atypia and nuclear density made it possible to diagnose them without endoscopic biopsy. Although endocytoscopic images closely correlated with conventional histology in the esophagus, appropriate preconditioning to constantly obtain sufficient image quality and universal criteria for endocytoscopic diagnosis of various diseases are essential before clinical application.

7. Endoscopic ultrasound

In physics, the term "ultrasound" applies to all sound waves with a frequency above the audible range of normal human hearing, about 20 kHz. The frequencies used in diagnostic ultrasound are typically between 2 and 18 MHz. A sound wave is typically produced by a piezoelectric transducer encased in a housing which can take a number of forms. Strong, short electrical pulses from the ultrasound machine make the transducer resonate at the desired frequency. The sound is focused either by the shape of the transducer, a lens in front of the transducer, or a complex set of control pulses from the ultrasound scanner. The wave travels into the body and comes into focus at a desired depth. The sound wave is partially reflected from the layers between different tissues. Specifically, sound is reflected anywhere there are density changes in the body: e.g., blood cells in blood plasma, small structures in organs, etc. Some of the reflections return to the same piezoelectric transducer that finally turns the vibrations once again into electrical pulses that will be processed and transformed into a digital image (Fig. 10).

Endoscopic ultrasound (EUS) was initially developed in the early 1980s primarily to overcome the limitations of transabdominal ultrasound in imaging the pancreas. In EUS, a small high-frequency ultrasound transducer is incorporated into the tip of a flexible endoscope.

The fundamental importance of EUS is its ability to provide information of the transmural status and layered framework of the GIT; mucosa through serosa and beyond.

7.1. Operating system

Radial scanning echoendoscopes were initially most frequently used for EUS. The ultrasound transducer rotates to provide a 360-degree cross-sectional image. Viewing frequencies between 5 and 20 MHz can be used. A balloon with water-filling capacity encases the ultrasound transducer at the tip of the endoscope. The water in the balloon helps overcome the difficulty of imaging in an air-filled lumen. Solid-state radial EUS instruments, without rotating parts, have been introduced more recently. Linear array echoendoscopes provide ultrasound images along the long axis of the echoendoscope. This type of echoendoscope provides a linear array view along the axis of the needle as is required for interventional EUS.

Endoscopic ultrasound provides a detailed view of the gastrointestinal wall layers, which appear as alternating bright and dark bands. These layers include (1) superficial mucosa (hyperechoic); (2) deep mucosa (hypoechoic); (3) submucosa (hyperechoic); (4) muscularis propria (hypoechoic); and (5) serosa (hyperechoic) (Fig. 11A and B).

Alternatively EUS can be performed using miniprobes and wire-guided catheter probes that can be inserted through the operative channel of conventional endoscope.

Today commercial 3D-EUS systems are available.

7.2. Clinical applications

EUS is classically indicated for the following GIT ailments;

(1) Staging of cancers; esophageal, pancreatic, gastric, bile duct, papilla of Vater, and rectum
(2) Evaluation of submucosal lesions
(3) Evaluation of extramural abnormalities
(4) Evaluation of pancreatic lesions
(5) Evaluation of thickened gastric folds
(6) Evaluation and EUS-guided FNA of lesions adjacent to esophagus, stomach, duodenum, and rectum
(7) Chronic pancreatitis
(8) Detection of common bile duct stones

When the gastrointestinal wall is examined with a miniprobe at higher frequencies (20 MHz), 9 endosonographic layers can be visualized [54] as shown in. The mucosa consists of 4 layers: 1st and 2nd layers represent the epithelium, 3rd layer lamina propria, and 4th layer being the muscularis mucosa. The 5th layer constituted by the submucosa, The muscularis propria contains three layers: the 6th layer is circular muscle, 7th layer is connective tissue between the circular and longitudinal muscle, and 8th layer is the longitudinal muscle. Finally, 9th layer is the adventitia. Hence, early and/or advanced histological changes in the GIT structures would be easily illustrated by EUS (Fig. 11).

EUS-guided FNA is increasingly being used for the diagnosis and staging of various cancers because it provides a minimally invasive alternative to surgical procedures to obtain tissue diagnosis and has a sensitivity and specificity that is better than or at least equal to radiographic imaging alone. EUS-guided FNA is more sensitive (88% vs. 57%) and specific (91% vs. 82%) than CT [54,55]. The accuracy of transrectal EUS for T staging ranges from 80% to 95%, compared with 65% to 75% for CT, and 75% to 85% for MRI [56,57]. Harewood and Wiersema [58] reported that the most cost-effective strategy for evaluation of non-metastatic rectal cancer was a combination of abdominal CT and transrectal EUS. In a prospective study of 80 patients with non-metastatic rectal cancer, EUS resulted in the change of management in 31% of the patients [59].

Another dimension of EUS is its therapeutic potential in a wide range of procedures, such as celiac plexus block, stent placement in pancreatic pseudocysts, failed CBD–pancreatic duct cannulations, and chemotherapy [60–62]. EUS has been used to perform celiac plexus block or neurolysis in patients with chronic pancreatitis and pancreatic cancer [63].

8. Conclusion

The usefulness and efficacy of the above-described technologies in the detection and cytological examination of

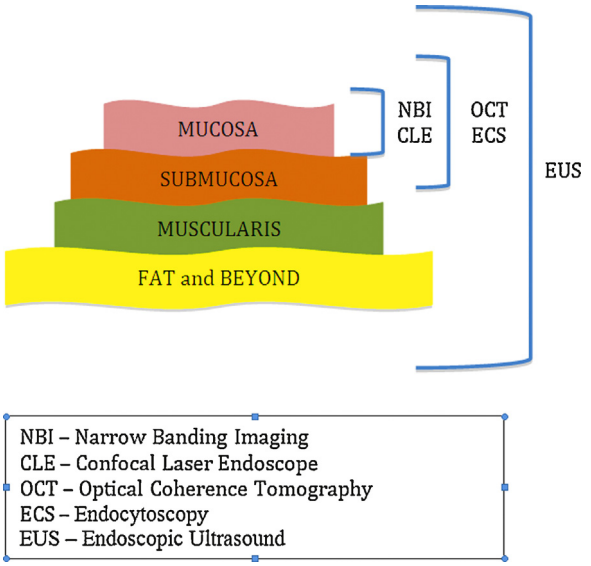

Fig. 12. Proper indication for advanced in vivo diagnostic technologies. A schematic diagram for the practical applications of the technologies in terms of GIT layers and mural thickness

the GIT abnormalities spring from the fact that they avoid repeat endoscopies, provide in vivo cytological diagnosis with accuracy, and help the treating physicians in timely planning of the multi-disciplinary strategy. A practical algorithm for the natural and logical application of these technologies is illustrated in (Fig. 12). This schematic diagram would certainly allow the physicians in selecting the appropriate investigation for the patients. More evidence-based research is needed to evaluate the global acceptance of these modern tools in terms of cost-effectiveness, feasibility, and the learning curve.

Conflict of interest

None declared.

Acknowledgement

The authors highly appreciate and value the contributions of Dr. Shaista Salman Guraya, Assistant Professor of Radiology Taibah University Saudi Arabia, in designing and crafting the figures in the manuscript.

References

[1] Parkin DM, Bray F, Ferlay J, Pisani P. Global cancer statistics, 2002. CA: A Cancer Journal for Clinicians 2005;55(2):74–108.
[2] Parkin DM, Bray F, Ferlay J, Pisani P. Estimating the world cancer burden: Globocan 2000. International Journal of Cancer 2001;94(2):153–6.
[3] Grady WM. Genetic testing for high-risk colon cancer patients. Gastroenterology 2003;124(6):1574–94.
[4] Guraya SY, Eltinay OE. Higher prevalence in young population and rightward shift of colorectal carcinoma. Saudi Medical Journal 2006;27(9):1391–3.
[5] Ciccolallo L, Capocaccia R, Coleman M, Berrino F, Coebergh J, Damhuis R, et al. Survival differences between European and US patients with colorectal cancer: role of stage at diagnosis and surgery. Gut 2005;54(2):268–73.
[6] Guraya SY. Modern oncosurgical treatment strategies for synchronous liver metastases from colorectal cancer. Journal of Microscopy and Ultrastructure 2013:1–7.
[7] Muto M, Katada C, Sano Y, Yoshida S. Narrow band imaging: a new diagnostic approach to visualize angiogenesis in superficial neoplasia. Clinical Gastroenterology and Hepatology 2005;3(7): S16–20.
[8] Machida H, Sano Y, Hamamoto Y, Muto M, Kozu T, Tajiri H, et al. Narrow-band imaging in the diagnosis of colorectal mucosal lesions: a pilot study. Endoscopy 2004;36(12):1094–8.
[9] van den Broek FJ, van Soest EJ, Naber AH, van Oijen AH, Mallant-Hent RC, Böhmer CJ, et al. Combining autofluorescence imaging and narrow-band imaging for the differentiation of adenomas from non-neoplastic colonic polyps among experienced and non-experienced endoscopists. The American Journal of Gastroenterology 2009;104(6):1498–507.
[10] Su M-Y, Hsu C-M, Ho Y-P, Chen P-C, Lin C-J, Chiu C-T. Comparative study of conventional colonoscopy, chromoendoscopy, and narrow-band imaging systems in differential diagnosis of neoplastic and nonneoplastic colonic polyps. The American Journal of Gastroenterology 2006;101(12):2711–6.
[11] Yeung T, Mortensen N. Advances in endoscopic visualization of colorectal polyps. Colorectal Disease 2011;13(4):352–9.
[12] Rastogi A, Pondugula K, Bansal A, Wani S, Keighley J, Sugar J, et al. Recognition of surface mucosal and vascular patterns of colon polyps by using narrow-band imaging: interobserver and intraobserver agreement and prediction of polyp histology. Gastrointestinal Endoscopy 2009;69(3):716–22.
[13] East J, Tan E, Bergman J, Saunders B, Tekkis P. Meta-analysis: narrow band imaging for lesion characterization in the colon, oesophagus, duodenal ampulla and lung. Alimentary Pharmacology & Therapeutics 2008;28(7):854–67.
[14] Gono K, Yamazaki K, Doguchi N, Nonami T, Obi T, Yamaguchi M, et al. Endoscopic observation of tissue by narrowband illumination. Optical Review 2003;10(4):211–5.
[15] Gono K, Obi T, Yamaguchi M, Ohyama N, Machida H, Sano Y, et al. Appearance of enhanced tissue features in narrow-band endoscopic imaging. Journal of Biomedical Optics 2004;9(3):568–77.
[16] Inoue T, Murano M, Murano N, Kuramoto T, Kawakami K, Abe Y, et al. Comparative study of conventional colonoscopy and pan-colonic narrow-band imaging system in the detection of neoplastic colonic polyps: a randomized, controlled trial. Journal of Gastroenterology 2008;43(1):45–50.
[17] Uraoka T, Saito Y, Ikematsu H, Yamamoto K, Sano Y. Sano's capillary pattern classification for narrow-band imaging of early colorectal lesions. Digestive Endoscopy 2011;23(s1):112–5.
[18] Sano Y, Ikematsu H, Fu KI, Emura F, Katagiri A, Horimatsu T, et al. Meshed capillary vessels by use of narrow-band imaging for differential diagnosis of small colorectal polyps. Gastrointestinal Endoscopy 2009;69(2):278–83.
[19] Katagiri A, Fu KI, Sano Y, Ikematsu H, Horimatsu T, Kaneko K, et al. Narrow band imaging with magnifying colonoscopy as diagnostic tool for predicting histology of early colorectal neoplasia. Alimentary Pharmacology & Therapeutics 2008;27(12):1269–74.
[20] Rex DK. Narrow-band imaging without optical magnification for histologic analysis of colorectal polyps. Gastroenterology 2009;136(4):1174–81.
[21] Ikematsu H, Matsuda T, Emura F, Saito Y, Uraoka T, Fu K-I, et al. Efficacy of capillary pattern type IIIA/IIIB by magnifying narrow band imaging for estimating depth of invasion of early colorectal neoplasms. BMC Gastroenterology 2010;10(1):33.
[22] van den Broek FJ, Fockens P, van Eeden S, Reitsma JB, Hardwick JC, Stokkers PC, et al. Endoscopic tri-modal imaging for surveillance in ulcerative colitis: randomised comparison of high-resolution endoscopy and autofluorescence imaging for neoplasia detection; and evaluation of narrow-band imaging for classification of lesions. Gut 2008;57(8):1083–9.
[23] Von Rückmann A, Fitzke FW, Bird AC. Fundus autofluorescence in age-related macular disease imaged with a laser scanning ophthalmoscope. Investigative Ophthalmology & Visual Science 1997;38(2):478–86.
[24] Kara MA, Peters FP, ten Kate FJ, van Deventer SJ, Fockens P, Bergman JJ. Endoscopic video autofluorescence imaging may improve the detection of early neoplasia in patients with Barrett's esophagus. Gastrointestinal Endoscopy 2005;61(6):679–85.
[25] Pohl H, Roesch T, Vieth M, Koch M, Becker V, Anders M, et al. Miniprobe confocal laser microscopy for the detection of invisible neoplasia in patients with Barrett's oesophagus. Gut 2008;57(12):1648–53.

[26] Kulapaditharom B, Boonkitticharoen V. Performance characteristics of fluorescence endoscope in detection of head and neck cancers. The Annals of Otology, Rhinology & Laryngology 2001;110(1):45–52.
[27] Betz C, Mehlmann M, Rick K, Stepp H, Grevers G, Baumgartner R, et al. Autofluorescence imaging and spectroscopy of normal and malignant mucosa in patients with head and neck cancer. Lasers in Surgery and Medicine 1999;25(4):323–34.
[28] Onizawa K, Okamura N, Saginoya H, Yoshida H. Characterization of autofluorescence in oral squamous cell carcinoma. Oral Oncology 2003;39(2):150–6.
[29] De Veld D, Witjes M, Sterenborg H, Roodenburg J. The status of in vivo autofluorescence spectroscopy and imaging for oral oncology. Oral Oncology 2005;41(2):117–31.
[30] Onizawa K, Yoshida H, Saginoya H. Chromatic analysis of autofluorescence emitted from squamous cell carcinomas arising in the oral cavity: a preliminary study. International Journal of Oral and Maxillofacial Surgery 2000;29(1):42–6.
[31] Arens C, Reussner D, Woenkhaus J, Leunig A, Betz C, Glanz H. Indirect fluorescence laryngoscopy in the diagnosis of precancerous and cancerous laryngeal lesions. European Archives of Oto-rhino-laryngology 2007;264(6):621–6.
[32] Kiesslich R, Burg J, Vieth M, Gnaendiger J, Enders M, Delaney P, et al. Confocal laser endoscopy for diagnosing intraepithelial neoplasias and colorectal cancer in vivo. Gastroenterology 2004;127(3):706–13.
[33] Swindle LD, Thomas SG, Freeman M, Delaney PM. View of normal human skin in vivo as observed using fluorescent fiber-optic confocal microscopic imaging. Journal of Investigative Dermatology 2003;121(4):706–12.
[34] McLaughlin RA, Sampson DD. Clinical applications of fiber-optic probes in optical coherence tomography. Optical Fiber Technology 2010;16(6):467–75.
[35] Drexler W, Fujimoto JG. Optical coherence tomography: technology and applications. Springer Adis US LLC; 2008.
[36] Drexler W, Chen Y, Aguirre A, Považay B, Unterhuber A, Fujimoto J. Ultrahigh resolution optical coherence tomography. Optical coherence tomography. Springer Adis US LLC; 2008. p. 239–79.
[37] Adler DC, Huang S-W, Huber R, Fujimoto JG. Photothermal detection of gold nanoparticles using phase-sensitive optical coherence tomography. Optics Express 2008;16(7):4376–93.
[38] Lee TM, Oldenburg AL, Sitafalwalla S, Marks DL, Luo W, Toublan FJ-J, et al. Engineered microsphere contrast agents for optical coherence tomography. Optics Letters 2003;28(17):1546–8.
[39] Tsuboi M, Hayashi A, Ikeda N, Honda H, Kato Y, Ichinose S, et al. Optical coherence tomography in the diagnosis of bronchial lesions. Lung Cancer 2005;49(3):387–94.
[40] Westphal V, Rollins AM, Willis J, Sivak Jr MV, Izatt JA. Correlation of endoscopic optical coherence tomography with histology in the lower-GI tract. Gastrointestinal Endoscopy 2005;61(4):537–46.
[41] Poneros JM, Brand S, Bouma BE, Tearney GJ, Compton CC, Nishioka NS. Diagnosis of specialized intestinal metaplasia by optical coherence tomography. Gastroenterology 2001;120(1):7–12.
[42] Bus M, Muller B, de Bruin D, Faber D, Kamphuis G, van Leeuwen T, et al. Volumetric in-vivo visualization of upper urinary tract tumors using optical coherence tomography: a pilot study. The Journal of Urology 2013:2236–42.
[43] Broecker EH, Dunbar MT. Optical coherence tomography: its clinical use for the diagnosis, pathogenesis, and management of macular conditions. Optometry: Journal of the American Optometric Association 2005;76(2):79–101.
[44] Motreff P, Levesque S, Souteyrand G, Sarry L, Ouchchane L, Citron B, et al. High-resolution coronary imaging by optical coherence tomography: feasibility, pitfalls and artefact analysis. Archives of Cardiovascular Diseases 2010;103(4):215–26.
[45] Georgakoudi I, Jacobson BC, Van Dam J, Backman V, Wallace MB, Müller MG, et al. Fluorescence, reflectance, and light-scattering spectroscopy for evaluating dysplasia in patients with Barrett's esophagus. Gastroenterology 2001;120(7):1620–9.
[46] Testoni PA, Mangiavillano B. Optical coherence tomography in detection of dysplasia and cancer of the gastrointestinal tract and bilio-pancreatic ductal system. World Journal of Gastroenterology: WJG 2008;14(42):6444.
[47] Fercher AF, Drexler W, Hitzenberger CK, Lasser T. Optical coherence tomography-principles and applications. Reports on Progress in Physics 2003;66(2):239.
[48] Xie T, Mukai D, Guo S, Brenner M, Chen Z. Fiber-optic-bundle-based optical coherence tomography. Optics Letters 2005;30(14):1803–5.
[49] Singh R, Sathananthan D, Tam W, Ruszkiewicz A. Endocytoscopy for diagnosis of gastrointestinal neoplasia: the expert's approach. Video Journal and Encyclopedia of GI Endoscopy 2013;1(1):18–9.
[50] Inoue H, Kudo S-E, Shiokawa A. Novel endoscopic imaging techniques toward in vivo observation of living cancer cells in the gastrointestinal tract. Clinical Gastroenterology and Hepatology 2005;3(7):S61–3.
[51] Kutsukawa M, Kudo S.-e., Ikehara N, Ogawa Y, Wakamura K, Mori Y, et al. Efficiency of endocytoscopy in differentiating types of serrated polyps. Gastrointestinal Endoscopy 2013:3575–80.
[52] Neumann H, Kiesslich R. Endomicroscopy and endocytoscopy in IBD. Gastrointestinal Endoscopy Clinics of North America 2013;23(3):695–705.
[53] Fujishiro M, Takubo K, Sato Y, Kaise M, Niwa Y, Kato M, et al. Potential and present limitation of endocytoscopy in the diagnosis of esophageal squamous-cell carcinoma: a multicenter ex vivo pilot study. Gastrointestinal Endoscopy 2007;66(3):551–5.
[54] Gutman J, Ullah A. Advances in endoscopic ultrasound. Ultrasound Clinics 2009;4(3):369–84.
[55] Toloza EM, Harpole L, McCrory DC. Noninvasive staging of non-small cell lung cancera review of the current evidence. CHEST Journal 2003;123(1 Suppl.):137S–46S.
[56] Kwok H, Bissett I, Hill G. Preoperative staging of rectal cancer. International Journal of Colorectal Disease 2000;15(1):9–20.
[57] Thaler W, Watzka S, Martin F, Giuseppe La Guardia M, Psenner K, Bonatti G, et al. Preoperative staging of rectal cancer by endoluminal ultrasound vs. magnetic resonance imaging. Diseases of the Colon & Rectum 1994;37(12):1189–93.
[58] Harewood GC, Wiersema MJ. Endosonography-guided fine needle aspiration biopsy in the evaluation of pancreatic masses. The American Journal of Gastroenterology 2002;97(6):1386–91.
[59] Harewood GC, Wiersema MJ, Nelson H, Maccarty RL, Olson JE, Clain JE, et al. A prospective, blinded assessment of the impact of preoperative staging on the management of rectal cancer. Gastroenterology 2002;123(1):24–32.
[60] Kaufman M, Singh G, Das S, Concha-Parra R, Erber J, Micames C, et al. Efficacy of endoscopic ultrasound-guided celiac plexus block and celiac plexus neurolysis for managing abdominal pain associated with chronic pancreatitis and pancreatic cancer. Journal of Clinical Gastroenterology 2010;44(2):127–34.
[61] Michaels AJ, Draganov PV. Endoscopic ultrasonography guided celiac plexus neurolysis and celiac plexus block in the management of pain due to pancreatic cancer and chronic pancreatitis. World Journal of Gastroenterology 2007;13(26):3575.
[62] Wiersema MJ, Wiersema LM. Endosonography-guided celiac plexus neurolysis. Gastrointestinal Endoscopy 1996;44(6):656–62.
[63] Levy MJ, Topazian MD, Wiersema MJ, Clain JE, Rajan E, Wang KK, et al. Initial evaluation of the efficacy and safety of endoscopic ultrasound-guided direct Ganglia neurolysis and block. The American Journal of Gastroenterology 2008;103(1):98–103.